J. Fluid Mech. (1993), *vol.* 252, *pp.* 117–145

Experimental investigation of wave boundary layers with a sudden change in roughness

By J. FREDSØE, B. M. SUMER, T. S. LAURSEN AND C. PEDERSEN

Technical University of Denmark, Institute of Hydrodynamics and Hydraulic Engineering, 2800 Lyngby, Denmark

(Received 9 December 1991 and in revised form 14 January 1993)

This study deals with turbulent oscillatory boundary-layer flows over a plane bed with a sudden spatial change in roughness. Two kinds of 'change in the roughness' were investigated: in one, the roughness changed from a smooth-wall roughness to a roughness equal to 4.8 mm, and in the other, it changed from a roughness equal to 0.35 mm to the same roughness as in the previous experiment (4.8 mm). The free-stream flow was a purely oscillating flow with sinusoidal velocity variation. Mean flow and turbulence properties were measured. The Reynolds number was 6×10^6 for the major part of the experiments, with a maximum velocity of approximately 2 m/s and the stroke of the motion about 6 m. The response of the boundary layer to the sudden change in roughness was found to occur over a transitional length of the flow. The bed shear stress over this transitional length attains a peak value over the bed section with the larger roughness. It was found that the amplification in the bed shear stress due to this peak could be up to 2.5 times its asymptotic value. Also, it was found that the turbulence is quantitatively different in the two half periods; a much stronger turbulence is experienced in the half period where the flow is towards the less-rough section. The present experiments further showed that a constant streaming occurs near the bed in the neighbourhood of the junction between the two bed sections. This streaming is directed towards the section with the larger roughness.

1. Introduction

Turbulent oscillatory boundary-layer flows have been investigated quite extensively in recent years. Theoretical models have been developed to cope with the mean-flow properties (Kajiura 1968; Bakker 1974; Grant & Madsen 1979; Fredsøe 1984, among others) and to compute the turbulence properties (Justesen & Fredsøe 1985; Hagatun & Eidsvik 1986; Justesen 1988, among others). Also, direct Navier–Stokes simulations of the turbulent oscillatory boundary-layer flows have been achieved over a fairly wide range of Reynolds number (Re) up to 5×10^5 where $Re = aU_m/\nu$, U_m is the maximum value of the free-stream velocity, a is the amplitude of the free-stream motion and ν is the kinematic viscosity (Spalart & Baldwin 1987).

On the experimental side, considerable insight has been gained on various aspects of the turbulent oscillatory boundary layers by the works of Hino, Kashiwayanagi, Nakayama & Hara (1983) and Sleath (1987). In Hino *et al.*'s work the boundary was smooth, while in Sleath's it was covered with sand, and both studies were conducted at relatively low Re numbers. Recently, an extensive experimental study has been conducted over both smooth and rough boundaries at high Re numbers up to $Re = 6 \times 10^6$ (Jensen, Sumer & Fredsøe 1989). The latter study was complementary to Hino

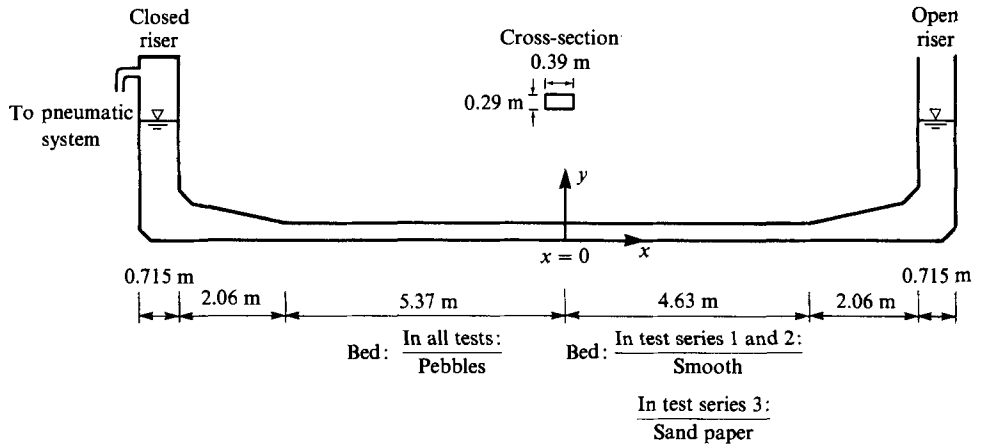

FIGURE 1. Test tunnel.

et al.'s work in the sense that the attention was concentrated on high-Re number flows, while it was complementary to Sleath's in the sense that the experiments were conducted at large values of the roughness parameter a/k_s ($0(10^3)$) in combination with large Reynolds number, k_s being the Nikuradse's equivalent sand roughness.

In all the previously mentioned investigations, the flow conditions were maintained uniform in the streamwise direction. Therefore there was no dependence of the boundary-layer properties on the streamwise distance.

The purpose of the present investigation is to study the response of the turbulent oscillatory boundary layer to a step change in bed roughness. Clearly, the boundary layer in the present case is no longer a uniform boundary layer; the boundary-layer properties depend not only on time and the vertical distance from the bed but also on the horizontal distance from the junction between the two bed sections. There have been several investigations regarding the response of a steady, turbulent boundary layer to a sudden change in wall roughness (Townsend 1966; Antonia & Luxton 1971, 1972; Andreopoulos & Wood 1982; Belcher, Xu & Hunt 1990; Tsujimoto, Urushizaki & Miyagaki 1991). The present work can be regarded as the extension of the preceding investigations to unsteady, turbulent boundary-layer flows.

The occurrence of situations where the bed roughness undergoes a sudden change can be of importance in several aspects: as one example, this type of flow is of engineering interest in relation to scour protection of structures in coastal areas. If this protection consists of stones laid on the seabed, a sudden change in roughness occurs from that of the original seabed to that of the stone protection. For the engineer it is important to know the increase in the bed shear stress on the stone protection in order to be able to design the size of the stones in the upper stone layer. Another example is the mechanics behind sediment sorting in coastal areas. The understanding of these mechanisms is rather poor at present. The induced streaming due to spatial variations in bed roughness as described in §5 in this paper must, however, be an important mechanism to smooth out spatial variations in grain sizes formed by different sorting mechanisms.

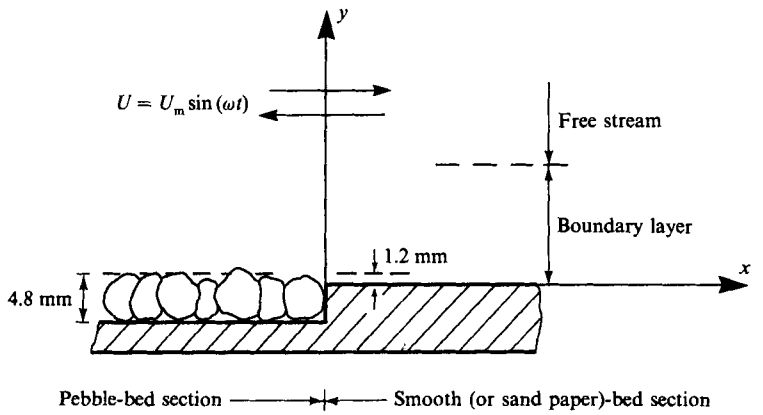

FIGURE 2. Definition sketch with the close-up picture of the junction of the two bed sections.

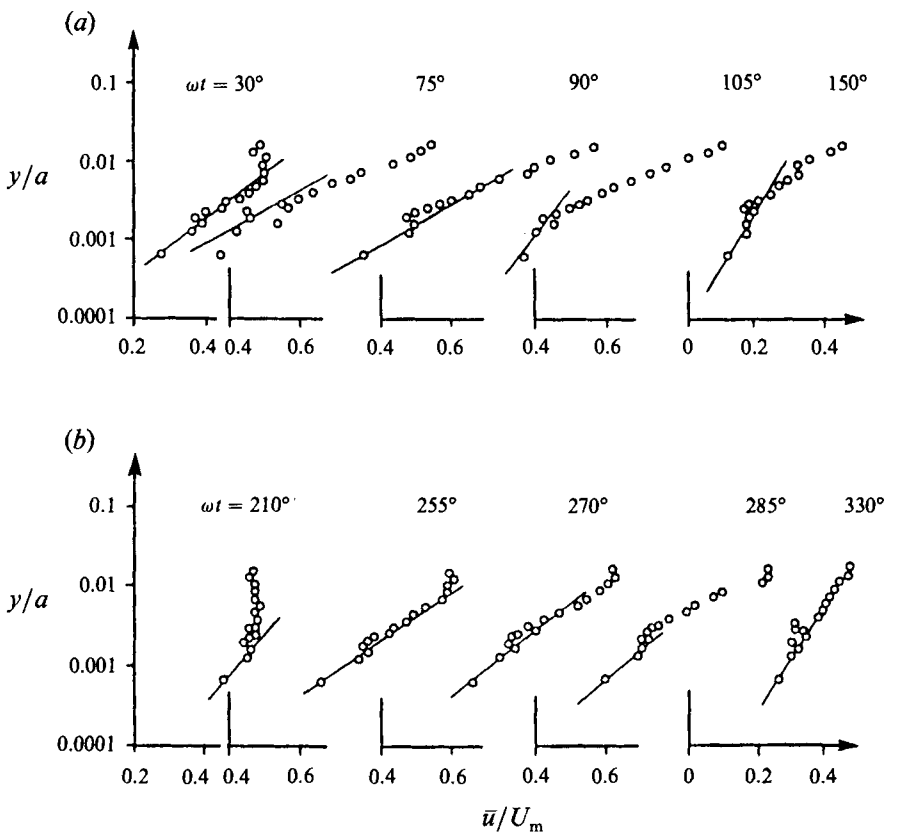

FIGURE 3. Mean streamwise velocity distribution in semi-log plot. Straight lines: log law, $\bar{u}/U_f = 2.5\ln(yU_f/\nu)+5$ for smooth bed and $\bar{u}/U_f = 2.5\ln(30y/k_s)$ for rough bed. (*a*) Flow from the rough (pebble) bed section to the smooth bed section. (*b*) Flow from the smooth bed to the rough (pebble) bed section. Test series 1. $x = 2.5$ cm.

2. Experimental set-up

The experiments were carried out in a U-shaped oscillatory-flow water tunnel. This tunnel is the same as that described by Jensen *et al.* (1989). The working section was

Test series	Bed configuration	Period (s)	U_m (m/s)	a (m)	$Re = aU_m/\nu$	k (mm)	k_s (mm)	a/k_s	Quantities measured	Apparatus	Number of cycles sampled	Sampling interval (ms)
1	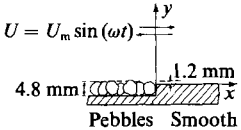	9.75	1.97	3.04	6×10^6	4.8 0	Pebbles 15 Smooth 0	200 ∞	$\bar{u}$, $(\overline{u'^2})^{\frac{1}{2}}$, $(\overline{v'^2})^{\frac{1}{2}}$, $\overline{u'v'}$ $\bar{\tau}_0$ only at Smooth	Two-component LDA Hot film	40	48
2	Ditto	9.75	0.57	0.88	5×10^5	4.8 0	Pebbles 15 Smooth 0	60 ∞	Ditto		40	48
3	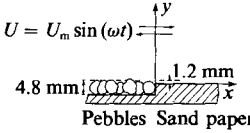	9.75	2.05	3.18	6.5×10^6	4.8 0.35	Pebbles 15 Sand paper 0.84	210 3800	$\bar{u}$, $(\overline{u'^2})^{\frac{1}{2}}$, $(\overline{v'^2})^{\frac{1}{2}}$, $\overline{u'v'}$	Two-component LDA	40	48

TABLE 1. Test conditions

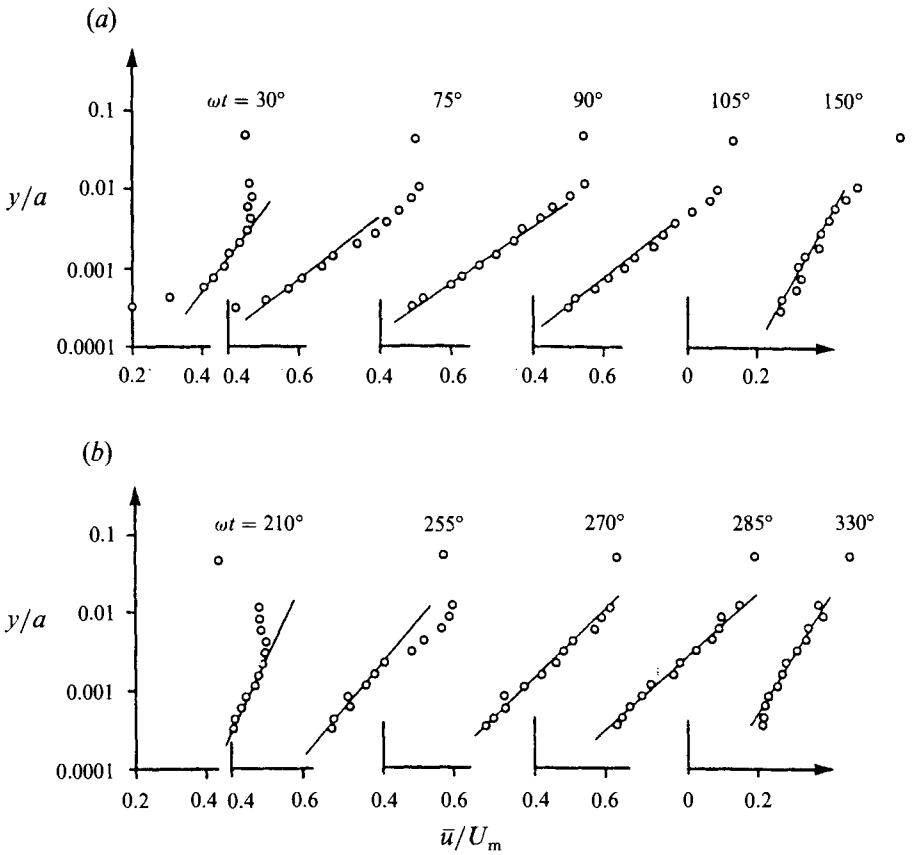

FIGURE 4. As figure 3. $x = 206$ cm.

10 m long and 0.39 m wide (figure 1). The top and side walls of the working section were made of smooth, transparent Perspex plates. The bottom wall over about half the length of the working section was maintained rough (the roughness being achieved by gluing pebbles), while the other part was smooth in test series 1 and 2 and it was covered with a sheet of sand paper in test series 3.

Regarding the pebble section of the bottom, pebbles of fairly uniform size were glued one layer deep to plastic plates, and these plastic plates were fixed rigidly to the bottom of the tunnel. The mean roughness height of the wall was $k = 4.8$ mm. Its k_s value (Nikuradse's equivalent sand roughness) was measured to be 15 mm (see §4).

For the smooth-bed section of the bottom (test series 1 and 2), PVC plates were fixed directly to the bottom of the tunnel. This was done in such a way that the level of the smooth bed section lay at a distance of $0.25k$ below the top of the roughness elements of the pebble-bed section (figure 2). The latter is the distance of the theoretical wall of a rough boundary from the top of the roughness elements, known from the steady boundary-layer flow research (Bayazit 1976).

Regarding the sand-paper experiments (test series 3), the smooth bed was simply covered with a sheet of sand paper, as mentioned previously. The roughness height of the sand paper was measured to be $k = 0.35$ mm, and the density of the protrusions was 80 grains/cm^2. This resulted in a Nikuradse's equivalent sand-roughness value of $k_s = 0.84$ mm (see §4).

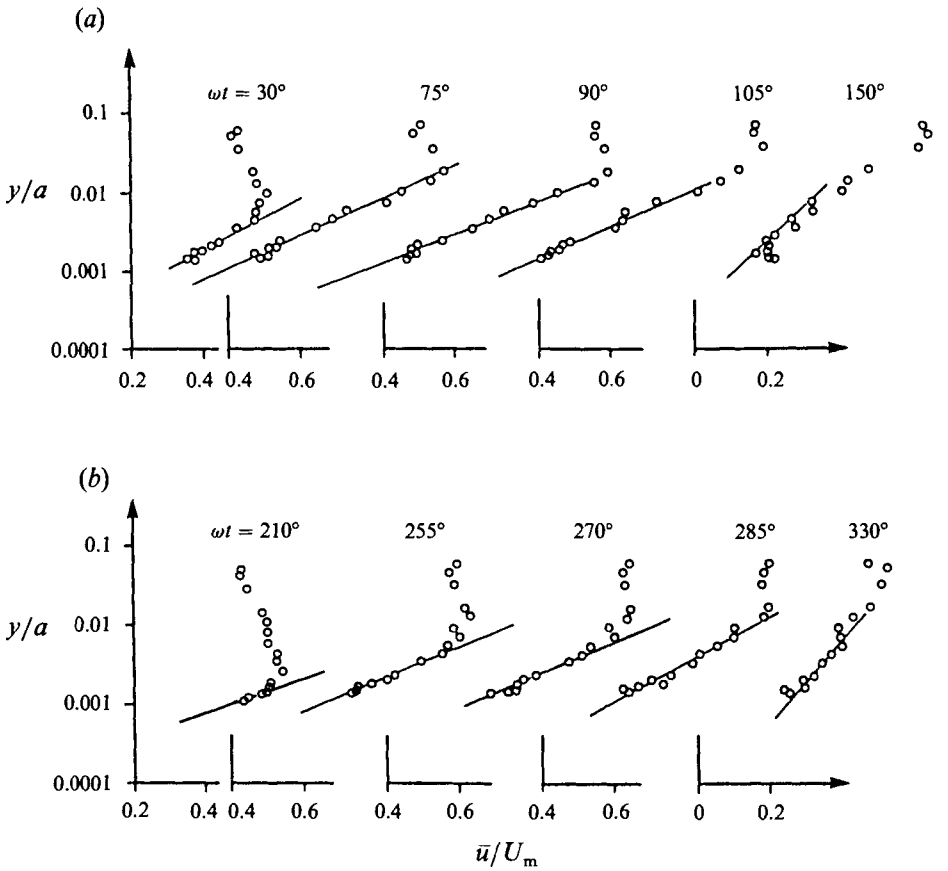

FIGURE 5. As figure 3. $x = -2.3$ cm.

The velocity distribution over the depth was measured by a two-component Dantec laser-Doppler anemometer (LDA). The LDA system was a Dantec two-colour high-performance fibre-optic system with a Dantec 60×11 fibre-optic probe head. A 100 mW argon laser was used in forward scatter mode with two Dantec 55N10 frequency shifters and two Dantec 55N20 frequency trackers, and also, in a few tests in back-scatter mode using two Dantec 57N10 burst spectrum analysers.

The bed shear stress was measured with a Dantec 55R46 hot-film probe. These measurements were conducted only at the smooth-bed section. The details of the measurements are exactly the same as described in Jensen *et al.* (1989).

Using a wave gauge, the water level in the open riser of the U-tube was recorded simultaneously with the velocity measurements. This served as a reference signal in the data processing.

Mean values of the quantities are calculated through ensemble averaging. The total number of cycles sampled and the sampling intervals are given in table 1.

3. Test conditions

The test conditions are summarized in table 1 where u and v are the flow velocities in the x- and y-directions (see figure 2), respectively, U_m is the maximum value of the free-stream velocity defined by

$$U = U_m \sin(\omega t). \tag{1}$$

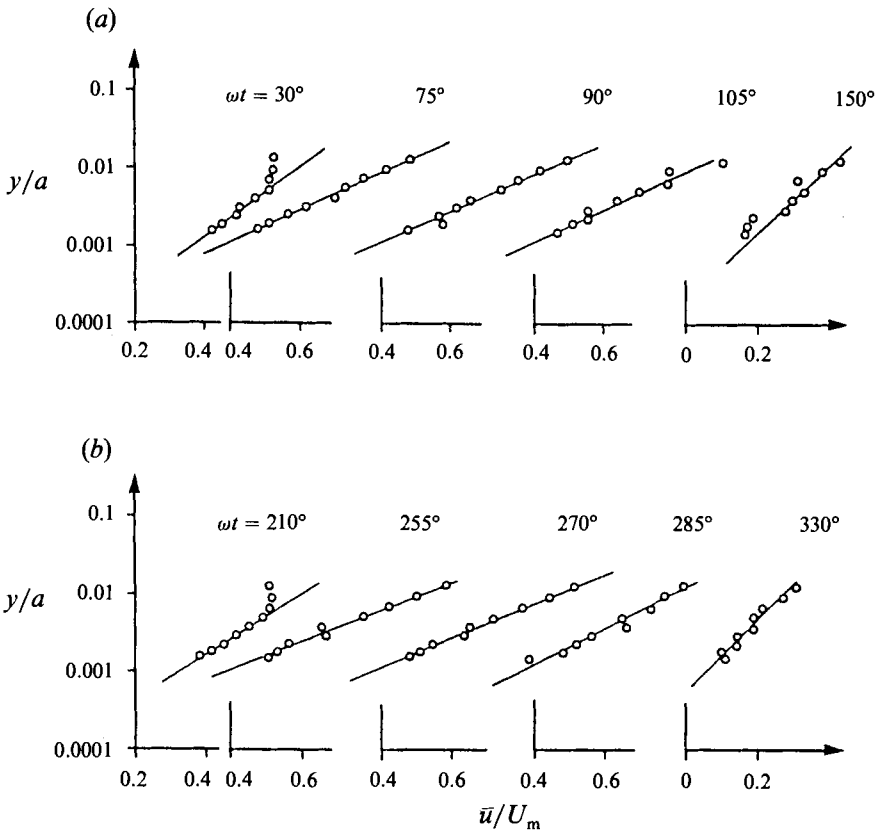

FIGURE 6. As figure 3. $x = -302$ cm.

Also in the table, a is the amplitude of the free-stream motion (equal to U_m/ω), ν is the kinematic viscosity, Re is the Reynolds number and τ_0 is the bed shear stress. The movement in the free-stream region was not absolutely symmetric in the two half periods; there was a slight difference between the maximum velocities in the two half periods. As a consequence of this, the period-averaged velocity in the free-stream region was measured to be non-zero, as will be shown later in figure 13. However, this value was found to be not larger than 1 cm/s (or in terms of U_m, not larger than 0.005 U_m) in the case of $Re \approx 6 \times 10^6$ tests. Also, the difference between the maximum velocities (experienced in the two half periods) itself was found to be not larger than $O(5$ cm/s) for the tests where $Re \approx 6 \times 10^6$ while it was found to be a factor 2 smaller than the latter in the case where $Re = 5 \times 10^5$. The U_m values in table 1 indicate the mean values of these maximum velocities experienced in the two half periods of the motion.

The velocity measurements were conducted at the following stations: $x = 2.5$, 5, 10, 20, 40 and 206 cm over the smooth-bed section and $x = -2.3$, -5, -20, -79 and -302 cm over the pebble-bed section in test series 1 and 2, and $x = 2.5$, 5, 10, 20, 40, 206 and 300 cm over the sandpaper-bed section and $x = -2.3$, -5, -10, -20, -79 and -302 cm over the pebble-bed section in test series 3.

The bed-shear-stress measurements on the other hand were made at the same x stations as in the velocity measurements along the smooth-bed section in test series 1.

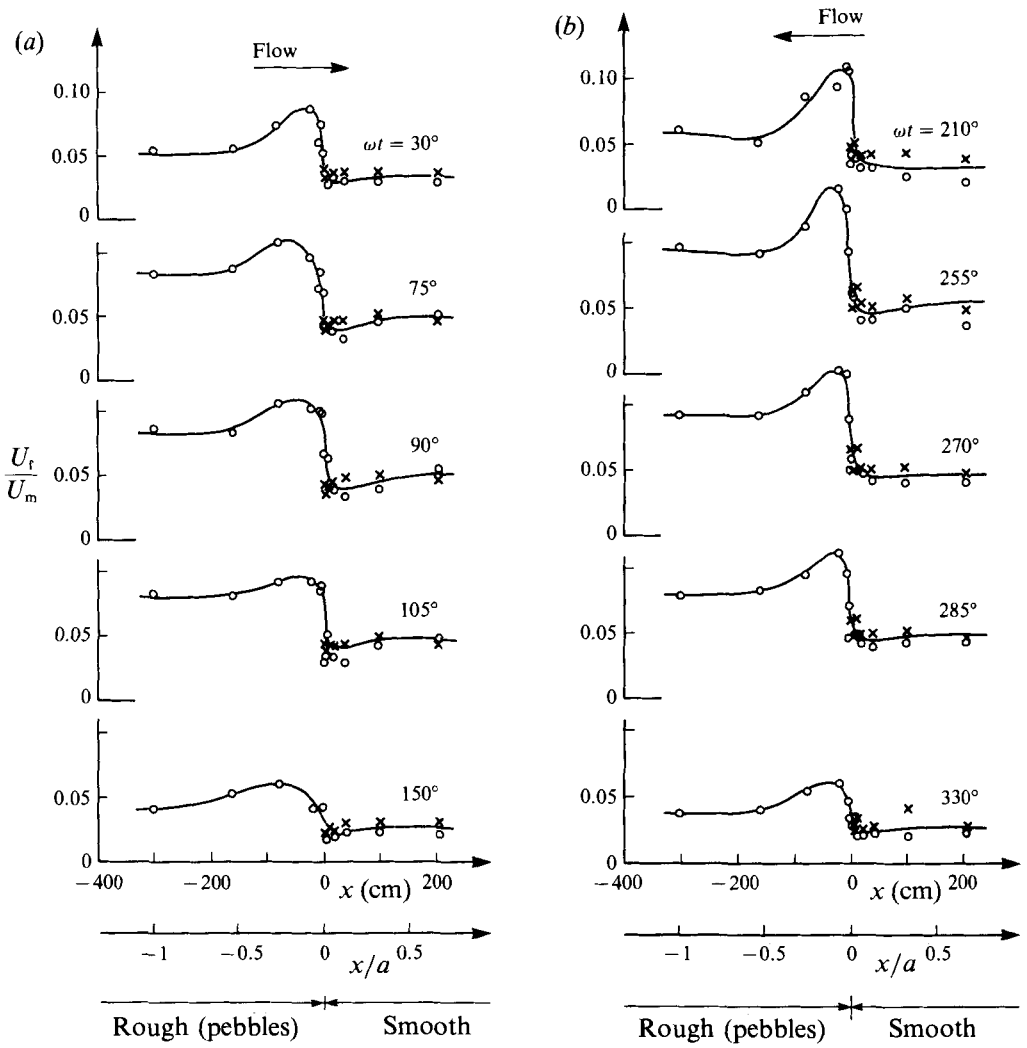

FIGURE 7. Time evolution of bed shear velocity, ○, logarithmic fit. ×, direct measurements. Test series 1.

4. Mean flow and the bed friction

Figures 3–6 present the mean velocity profiles over one period of the motion for four measurement stations in test series 1; two of the stations lie in the smooth-bed section and the other two in the rough-bed section.

Figure 7 illustrates how the bed shear stress evolves with time in test series 1. The bed shear-stress velocity, U_f, is defined by

$$U_f = \left(\frac{\bar{\tau}_0}{\rho}\right)^{\frac{1}{2}}. \tag{2}$$

U_f was obtained in two ways: (*a*) by fitting straight lines to the logarithmic-layer portion of the mean velocity distribution (see figures 3–6) and (*b*) by direct measurements (only for the smooth-wall section). The former gave also the Nikuradse's

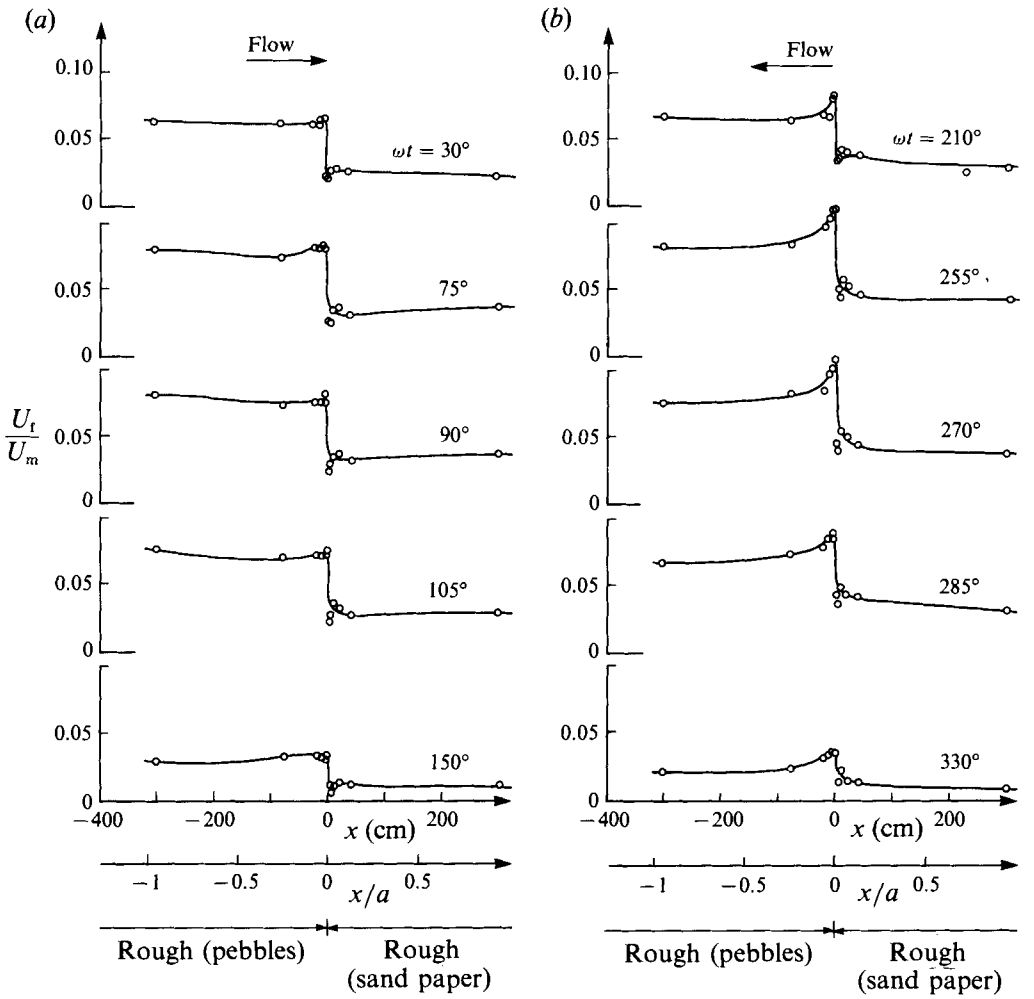

FIGURE 8. Time evolution of bed shear stress velocity. Test series 3.

equivalent sand roughness k_s of the rough boundary under consideration. As is seen from the figure, the agreement between the two methods is satisfactory.

Figure 8 depicts the corresponding results obtained in test series 3 where the smooth wall was replaced with the sand-paper covered wall.

Clearly, the bed shear stress is larger in the rough-bed section than in the smooth-bed section in figure 7, as expected. The same is also true for figure 8 where the shear stress over the larger roughness (pebble) section is greater than over the smaller roughness (sand-paper) section. However, figures 7(*b*) and 8(*b*) indicate that the bed shear stress attains a strong peak value over the pebble-bed section near $x = 0$ before it assumes its asymptotic value as $x \to -\infty$. It should be noted that the steady boundary-layer research regarding the response of a boundary layer to a step change in roughness has indicated exactly the same kind of behaviour. In Antonia & Luxton's (1971) work, for example, the wall shear stress was determined over the rough-wall section, using two independent methods. The peak value of the shear stress was found to be 1.7 times larger than the undisturbed, rough-wall shear stress value according to the one method, and this factor was found to be 3.3 according to the other method.

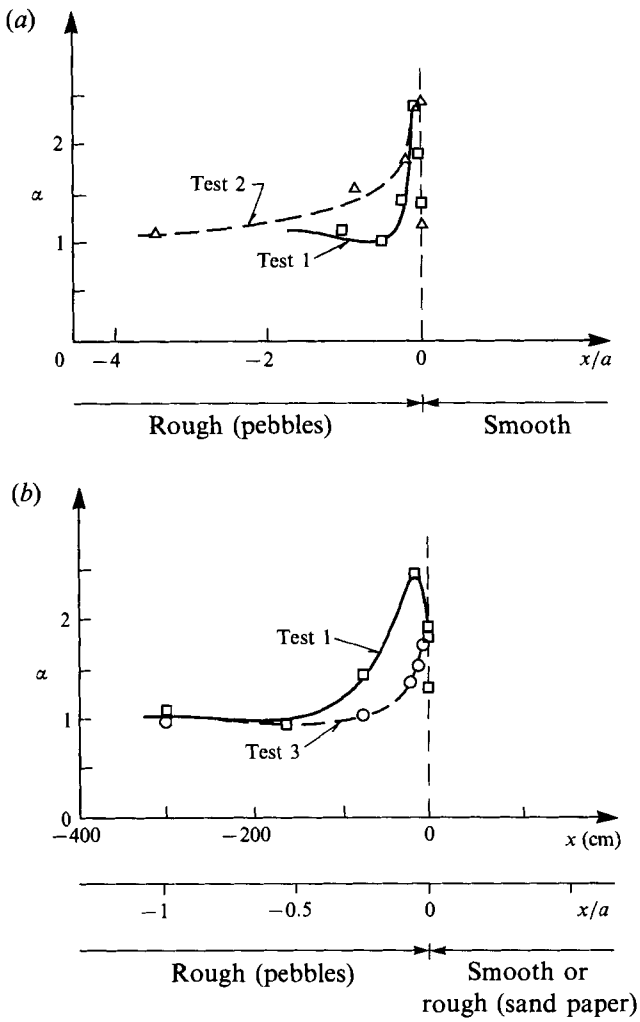

FIGURE 9. Amplification factor regarding the bed shear stress over the pebble bed section. (*a*) Test series 1 and 2. Pebble/smooth. (*b*) Test series 1 (pebble/smooth) and test series 3 (pebble/sand paper).

This peak in the bed shear stress is associated with the occurrence of a non-zero vertical mean flow near $x = 0$ over the pebble section, as will be shown in §5.

Figure 9 illustrates how much the bed shear stress is amplified owing to the above-mentioned peak with respect to its undisturbed value. The results of test 1 are included in both figure 9(*a*) and figure 9(*b*) to facilitate comparison. Here α, the amplification factor, is defined by

$$\alpha = \frac{\text{Max}\{U_f^2\}}{U_{fm}^2} = \frac{\text{Max}\{\bar{\tau}_0\}}{\bar{\tau}_{0m}}, \tag{3}$$

in which $\bar{\tau}_{0m}$ is the maximum value of the undisturbed bed shear stress over the pebble-bed section and $\text{Max}\{\bar{\tau}_0\}$ is the maximum value of the bed shear stress experienced over the pebble-bed section. As implied by the definition, $\bar{\tau}_{0m}$ is the maximum undisturbed bed shear stress over time, while $\text{Max}\{\bar{\tau}_0\}$ is the maximum value of $\bar{\tau}_0$ over x. As seen

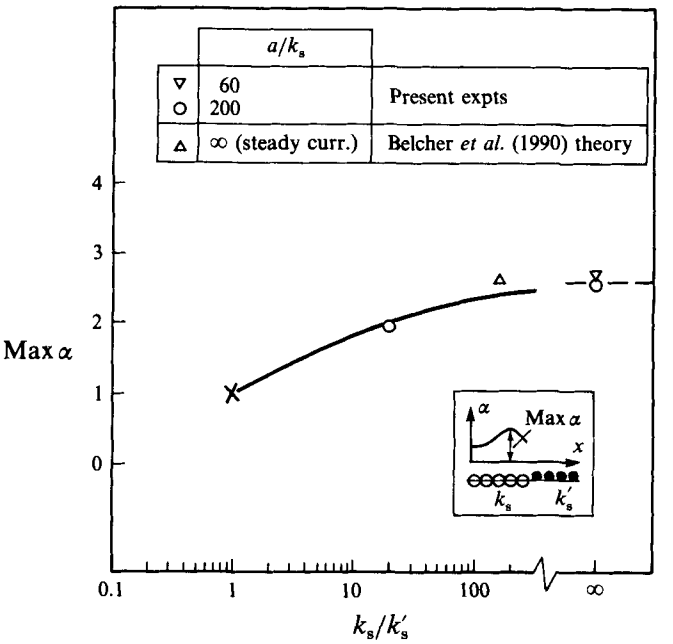

FIGURE 10. Maximum amplification factor regarding the bed shear stress. ○, test series 1 and 3. ▽, test series 2. ×, the case where the bed has a uniform roughness.

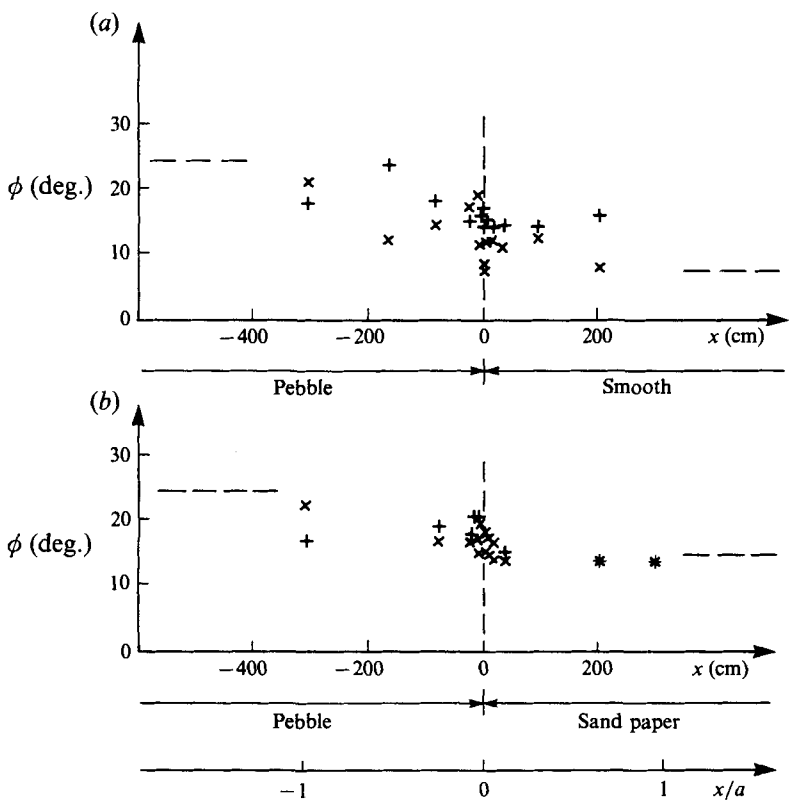

FIGURE 11. Phase lead of the near-wall velocity over the free-stream velocity. (*a*) Test series 1 and (*b*) test series 3. +, near-wall flow is occurring from pebble section to smooth-wall or to sand-paper section; ×, otherwise; – – –, asymptotic values, phase lead of the bed shear stress over the free-stream velocity: from Jensen *et al.* (1989); Jensen (1989).

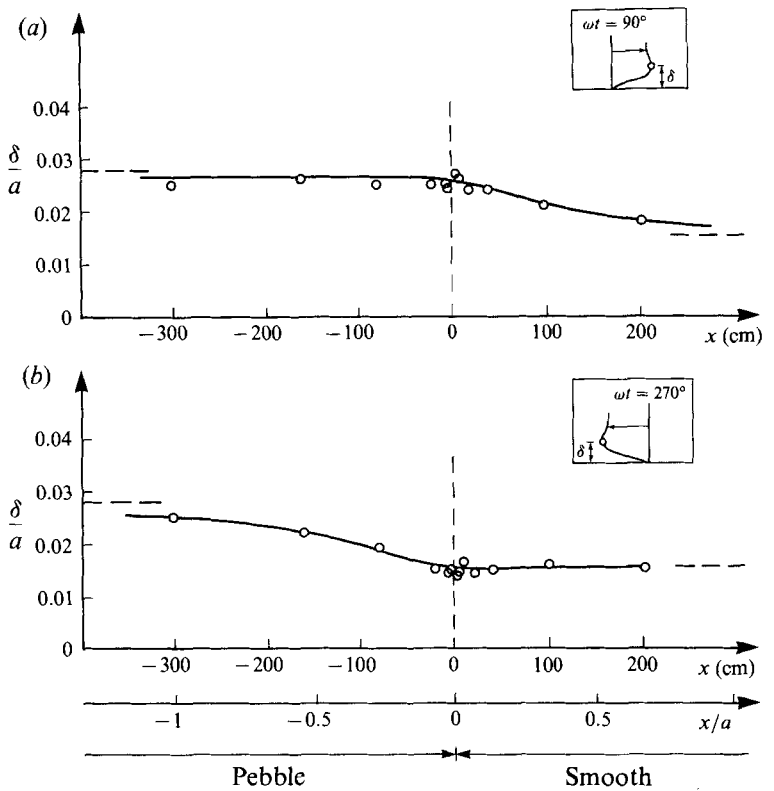

FIGURE 12. Boundary-layer thickness (*a*) in the rough-to-smooth half period and (*b*) in the smooth-to-rough half period. Test series 1. ---, asymptotic values for completely rough and completely smooth beds: from Jensen *et al.* (1989).

from the figure, the maximum amplification in the shear stress is about 2.5 for the pebble/smooth bed tests and about 1.8 for the pebble/sand paper bed tests.

Figure 10, on the other hand, presents the maximum amplification factor as a function of the roughness ratio k_s/k_s' where k_s is the larger roughness and k_s' is the smaller roughness. From dimensional considerations, Max α may depend on the following two parameters

$$\text{Max}\,\alpha = f\left(\frac{k_s}{k_s'}, \frac{a}{k_s}\right). \tag{4}$$

Obviously, Max α will attain its largest value, as the ratio $k_s/k_s' \to \infty$. Figure 10 includes also Belcher, Xu & Hunt's (1990) theoretical result obtained for steady current ($a/k_s = \infty$). It may be argued that the steady-flow solutions should be a fair approximation to the unsteady flow at the time in the cycle when the acceleration is zero (in the neighbourhood of $\omega t = 90°$ and 270°). Indeed, previous work for uniform oscillatory boundary layers (Jensen *et al.* 1989) revealed this with regard to the mean velocity distribution as well as the distributions of turbulence quantities. Therefore a comparison between the present results and Belcher *et al.*'s theoretical result can be made. In Belcher *et al.*'s study the flow and the bed shear stress were obtained through a perturbation analysis for an arbitrary variation of surface roughness, and then the theory was applied to two special cases, one of which was the case of a step change in roughness with the parameter $M = \ln(z_1/z_0) = -4.83$ where z_0 and z_1 are the

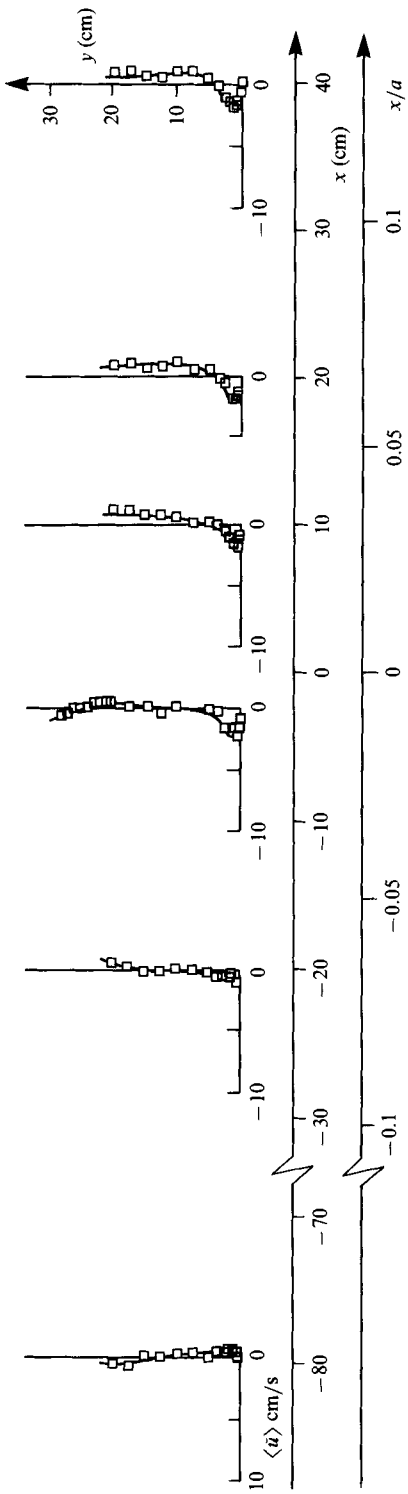

FIGURE 13. Period-averaged velocity distributions in the test section with no spatial variation in bed roughness (completely smooth bed). Test conditions are the same as in test series 1.

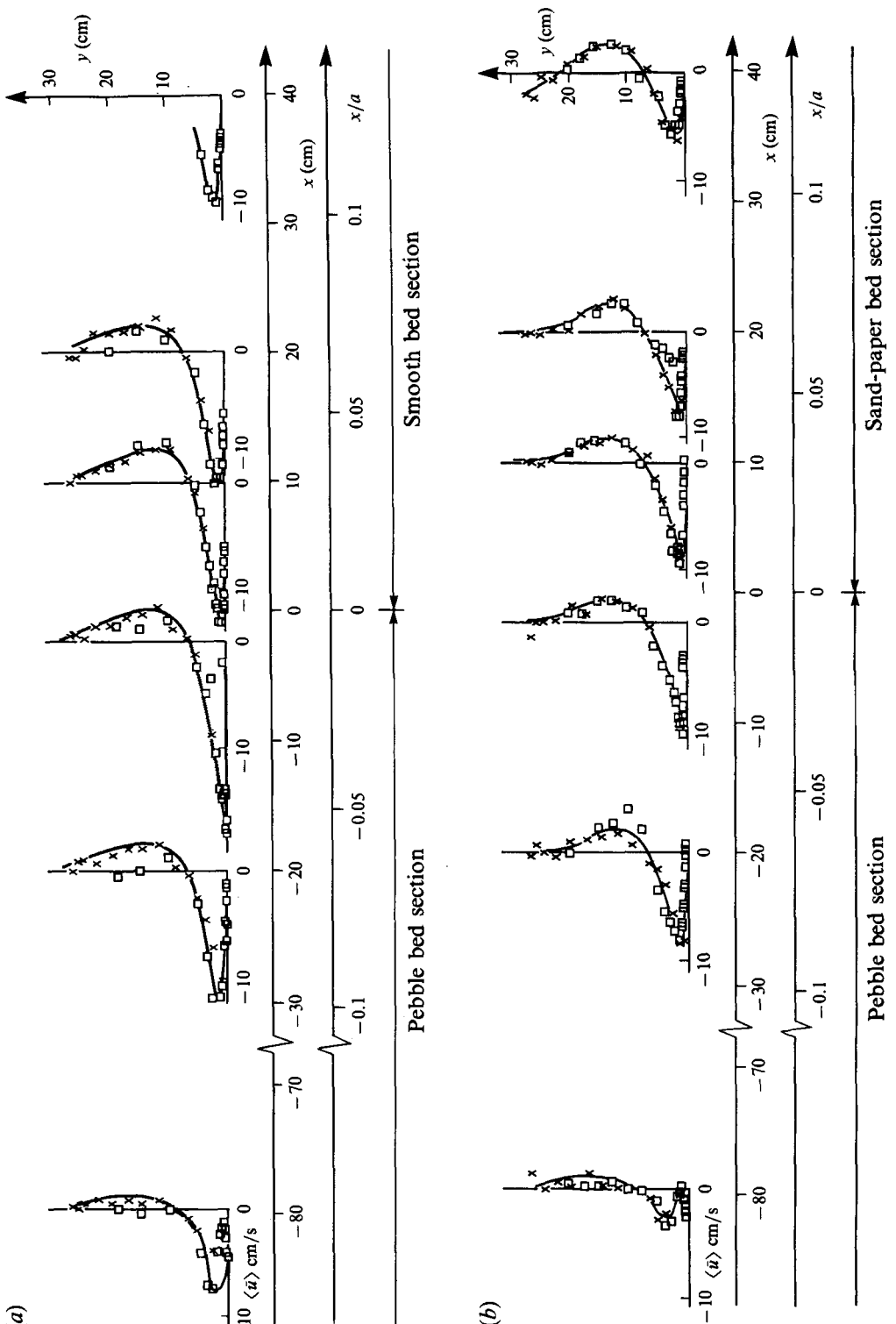

FIGURE 14. Period-averaged velocity distributions. Streaming. (*a*) Rough (pebbles)/smooth bed. Test series 1. (*b*) Rough (pebbles)/rough (sand-paper) bed. Test series 3. □, forward scatter measurements; ×, back-scatter measurements.

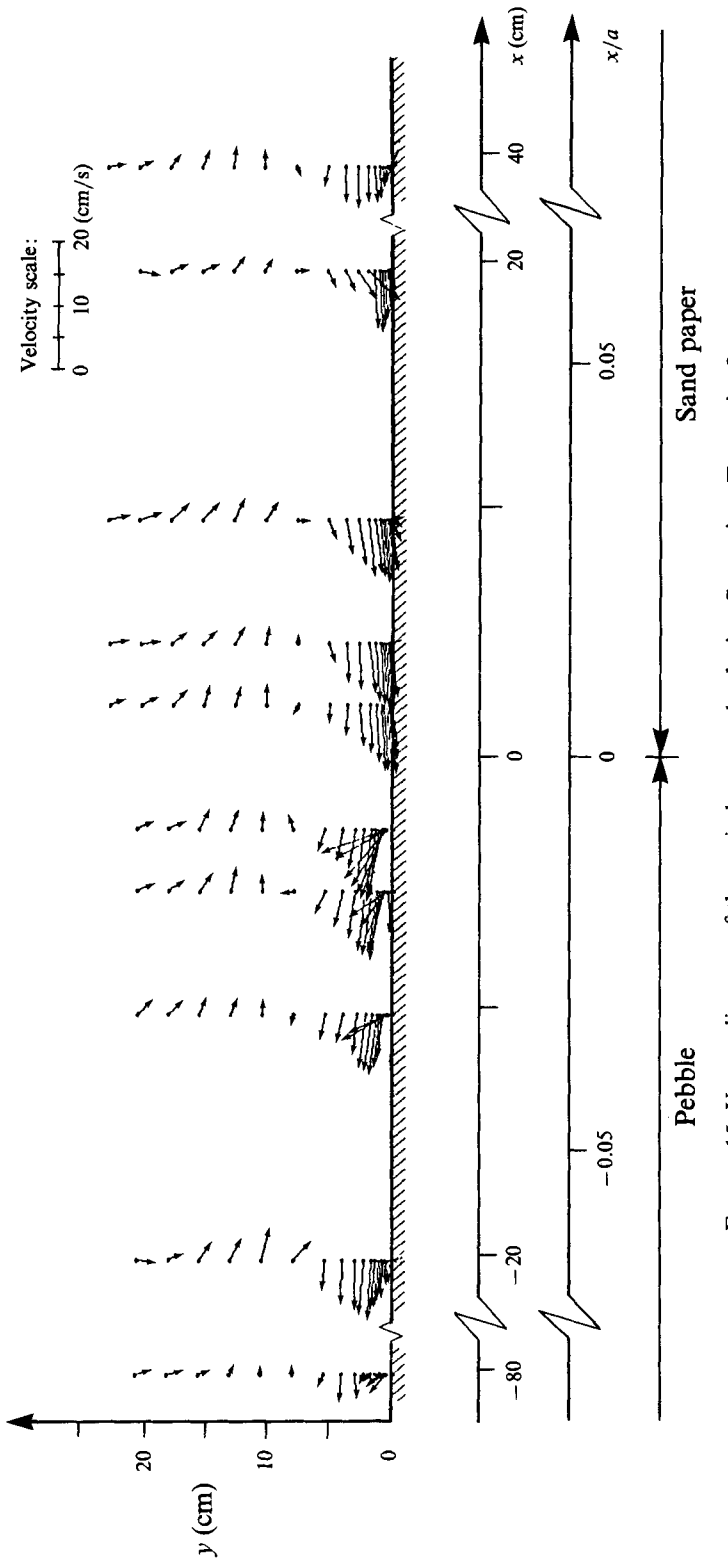

FIGURE 15. Vector diagram of the period-averaged velocity. Streaming. Test series 3.

roughness lengths before and after the step change in the roughness (the latter gives a roughness ratio $z_1/z_0 = k_s/k_s' = 125$). It was found that the theory agreed well with Bradley's (1968) steady-current experiments. Figure 10 indicates that the present experimental results are consistent with Belcher *et al.*'s theoretical result.

When considering Belcher *et al.*'s steady-current point in figure 10 and the point which represents the bed with a uniform roughness (the cross in the figure), one may conclude that the variation of Max α with k_s/k_s' in the case of steady currents will not be extremely different from that obtained in oscillatory flows (the solid curve in figure 10). Hence, one may deduce from the figure that while the amplification in the shear stress caused by a step change in the roughness ranges from 1 to 2.5, the maximum amplification is around 2.5, no matter whether the flow is a steady current or an oscillatory flow.

It is known that the bed shear stress leads over the free-stream velocity in the phase space. This phase lead was found to be approximately 7° for smooth beds for Re of 6×10^6 and 12° for the sand-paper roughened bed for the same Re number (Jensen *et al.* 1989). Figure 11 depicts the phase information obtained in the present study. Here ϕ is the phase lead of the streamwise velocity measured at the point nearest the bed over the free-stream velocity. Note that the nearest point to the bed was located at about $y = 1$ mm over the smooth bed and also over the sand-paper bed and it was located at about $y = 4$ mm over the pebble bed where y is measured from the theoretical wall. As is seen from the figure, the present findings reconcile well with the asymptotic values obtained by Jensen *et al.* (1989).

Finally, figure 12 depicts the variation of the boundary-layer thickness as a function of the streamwise distance. The boundary-layer thickness δ is defined in the same manner as in Jensen *et al.* (1989); namely, δ is the distance from the bed of the level where the overshooting velocity profile has its maximum at the phase value $\omega t = 90°$ for the rough-to-smooth half period and at $\omega t = 270°$ for the smooth-to-rough half period, as indicated in the figure. As expected, the transition regarding the boundary-layer thickness takes place over a length which covers a range from $x/a = 0$ to about $x/a = 1$ in the rough-to-smooth half period and that from $x/a = 0$ to about $x/a = -1$ in the smooth-to-rough half period.

5. Streaming near the bed

It is well known that in the non-uniform wave boundary layers, the period-averaged velocity $\langle \bar{u} \rangle$, defined by

$$\langle \bar{u} \rangle = \frac{1}{T} \int_0^T \bar{u} \, \mathrm{d}t, \tag{5}$$

becomes different from zero. Here, T is the period of the oscillatory flow. Longuet-Higgins (1957) calculated the streaming under sinusoidal waves due to the non-uniformity of the wave boundary layer caused by the spatial changes of the orbital velocities in real waves (in contrast to the oscillatory flow in uniform pipes, etc.). The streaming is introduced also in the present case; however, the non-uniformity in the present case is caused by the spatial variation in roughness.

5.1. *Period-averaged flow in the test section with uniform bed roughness*

In order to assess the significance of the streaming caused by the spatial variation in roughness, first the period-averaged velocity profiles were measured at several measurement stations in the tunnel under uniform bed-roughness condition where the

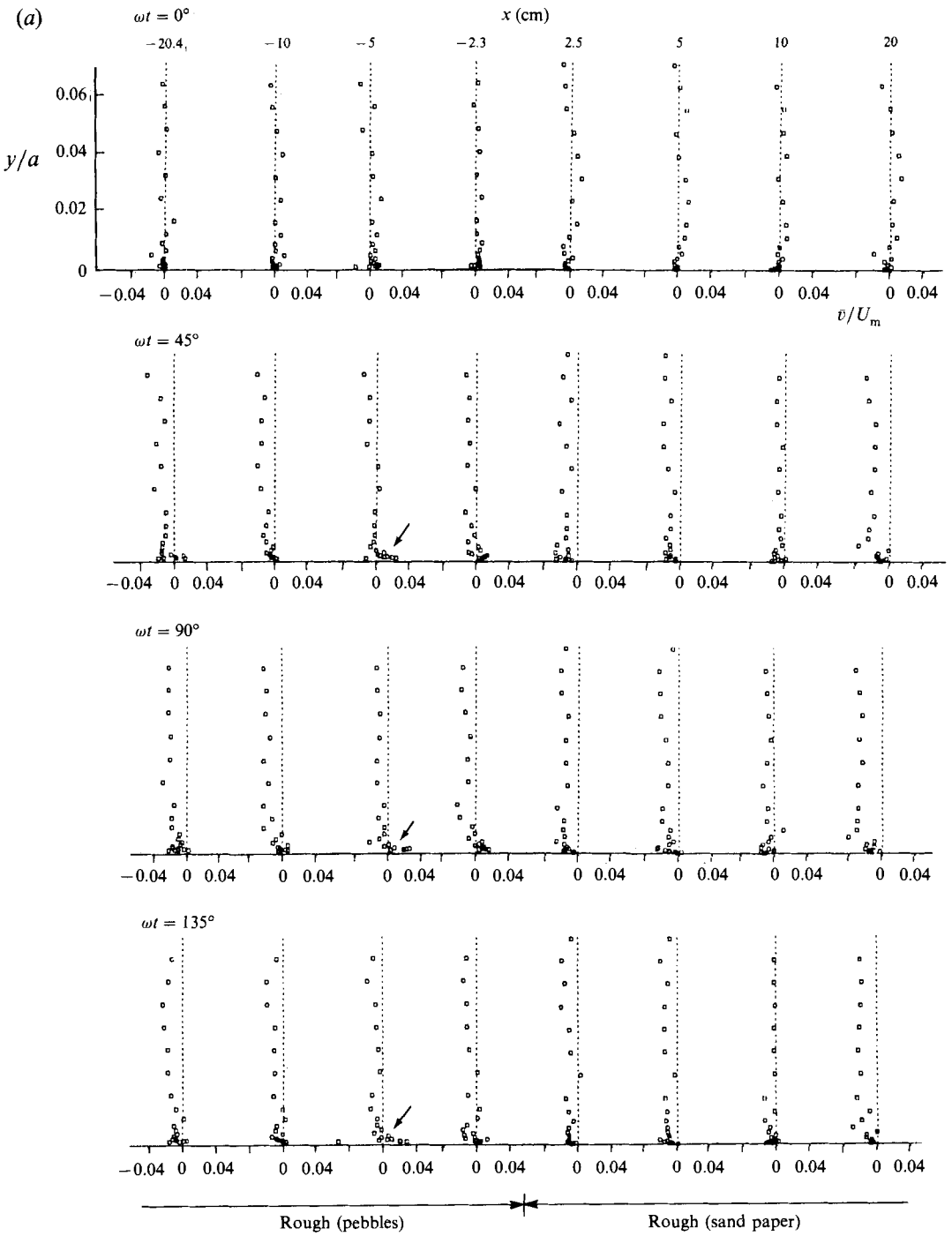

FIGURE 16(*a*). For caption see next page.

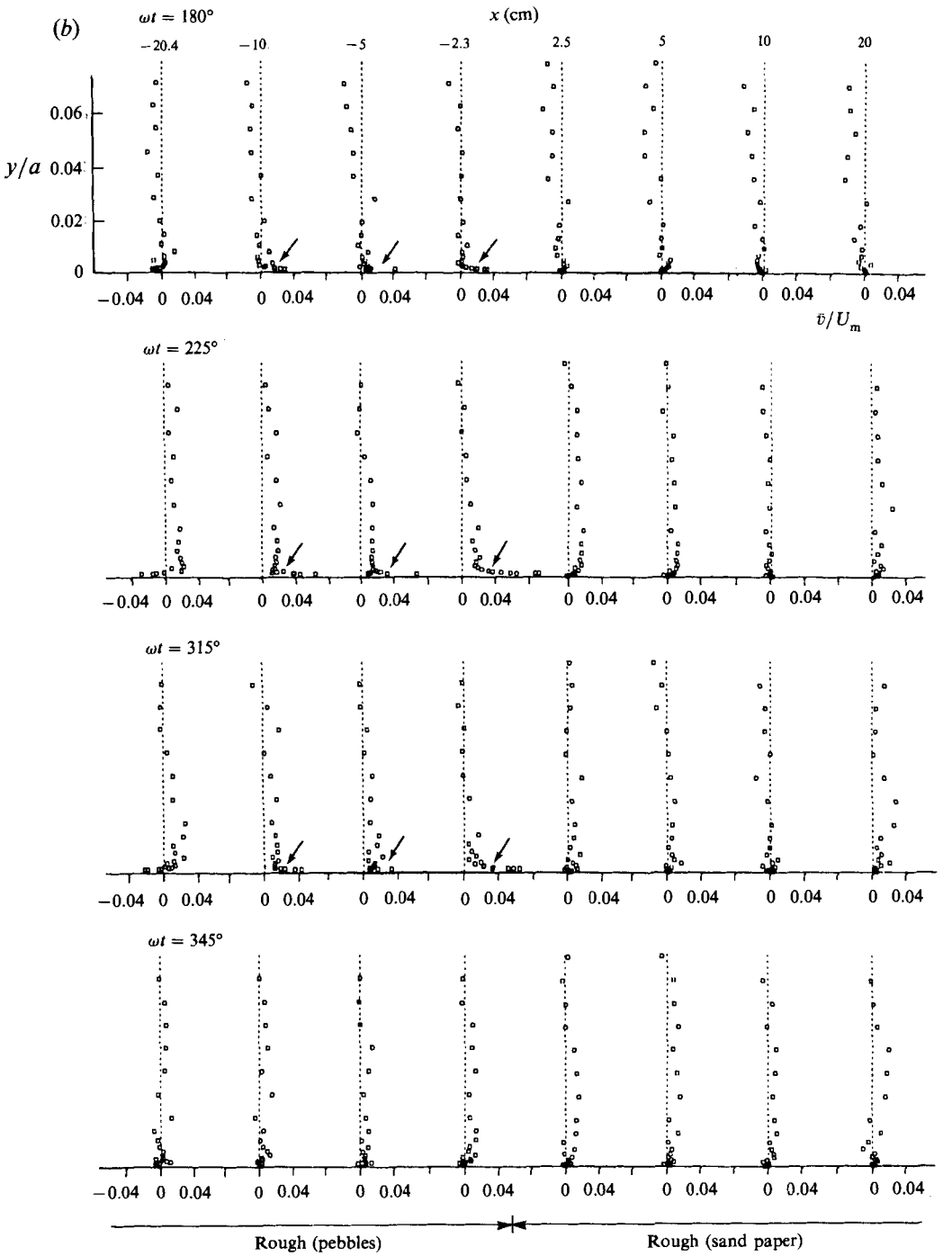

FIGURE 16. Mean vertical velocity distributions test series 3. (*a*) Flow from the pebble bed section to the sand-paper bed section. (*b*) Flow from the sand-paper bed section to the pebble bed section.

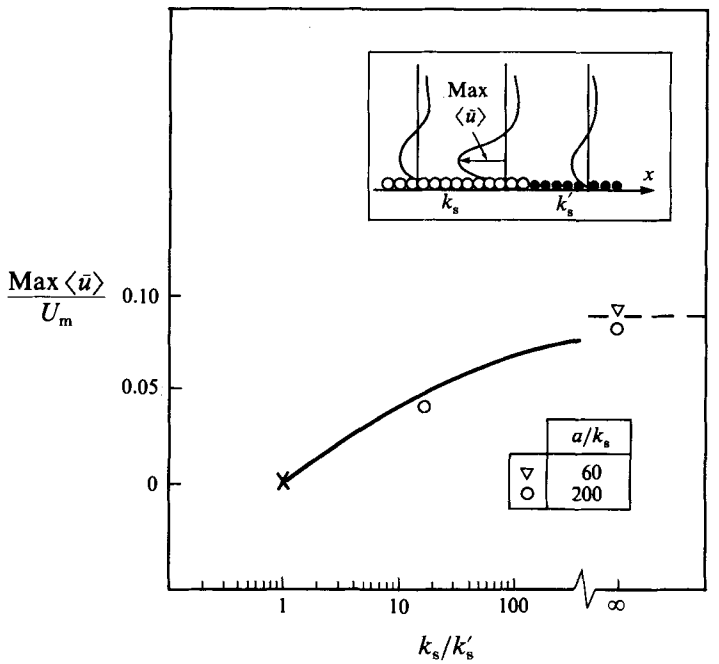

FIGURE 17. Maximum streaming velocity. ○, test series 1 and 3. ▽, test series 2. ×, the case where the bed has a uniform roughness.

bed was completely smooth. In these experiments the flow conditions were maintained the same as in test 1.

The measured velocity profiles are depicted in figure 13. The scales in the figure are maintained the same as in figure 14 where the corresponding velocity profiles are presented for test series 1 and 3 so that comparison can be made on the same basis. Figure 13 indicates that there is a secondary circulation in the test section. The data in the figure shows that the streaming near the bed associated with this circulation is not larger than 1 % of the maximum velocity of the motion (cf. table 1). Experiments done under exactly the same flow conditions as in test series 2, but with this uniform bed roughness (namely the smooth bottom), have given similar results.

This secondary circulation is caused by the presence of the contraction sections at the two ends of the tunnel. As is shown in Sumer, Laursen and Fredsøe (1993) in conjunction with oscillatory boundary-layer flows in convergent–divergent channels, the presence of such convergent–divergent sections would cause a streaming near the walls in the direction towards the convergent section.

Figure 13 further indicates that the reversal of the near-wall flow occurs somewhere between $x = -20$ cm and $x = -80$ cm. This coincides with the mid-section of the tunnel (cf. figure 1), and this behaviour must in fact be expected, owing to symmetry.

5.2. *Streaming induced by the spatial variation of bed roughness*

Figures 14(*a*) and 14(*b*) present the period-averaged velocity profiles in the case of pebble bed/smooth bed (test series 1) and also in the case of sand-paper bed/smooth bed (test series 3), respectively. Comparison of figures 14(*a*) and 14(*b*) with figure 13 indicates that a strong streaming of fluid occurs near the bed by the introduction of a step change in the bed roughness. As can be seen, this streaming occurs in the direction

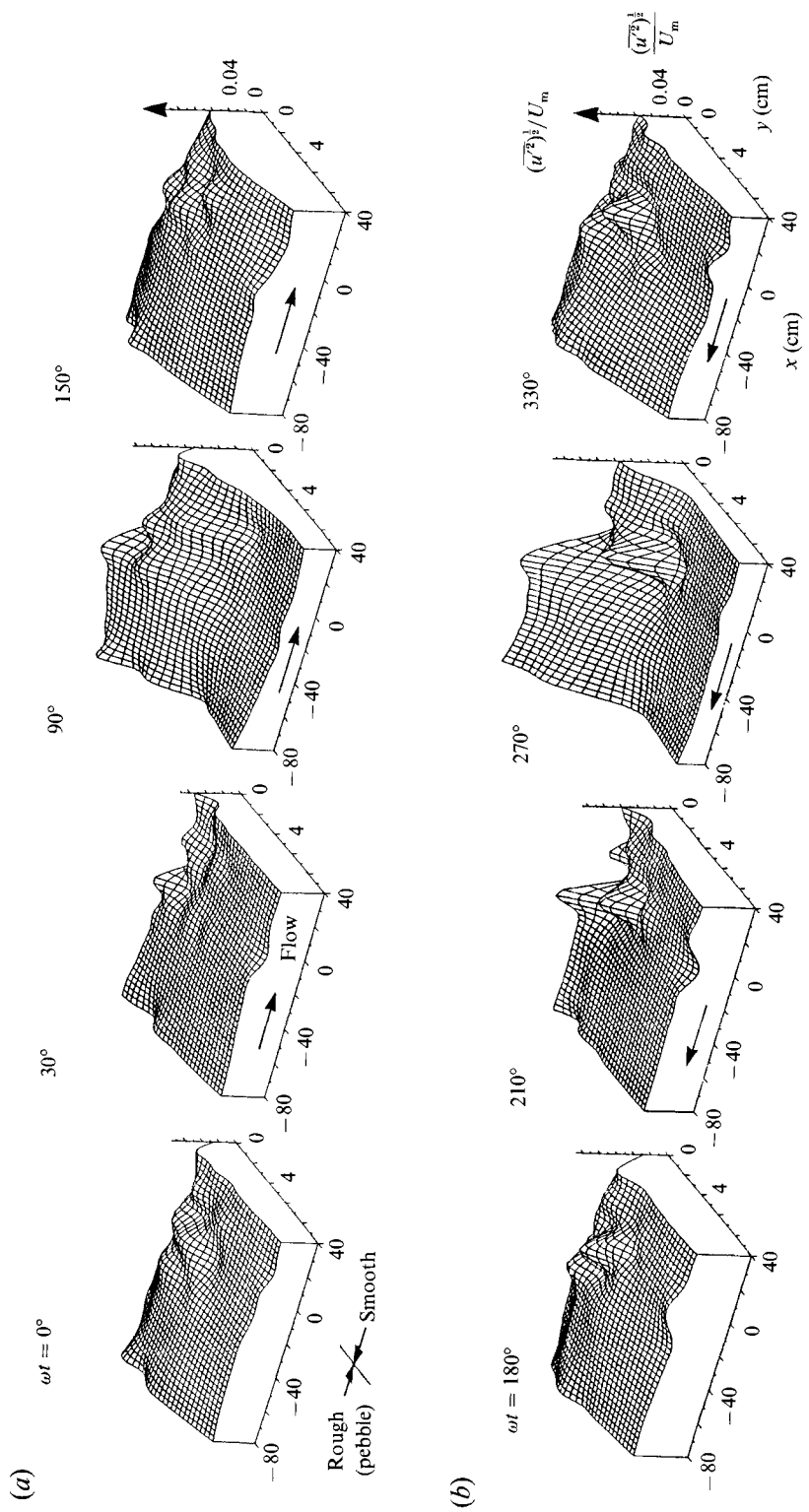

FIGURE 18. Root mean square value of u'. Test series 1. (*a*) Flow from the rough (pebble) bed section to the smooth bed section. (*b*) Flow from the smooth bed section to the rough (pebble) bed section.

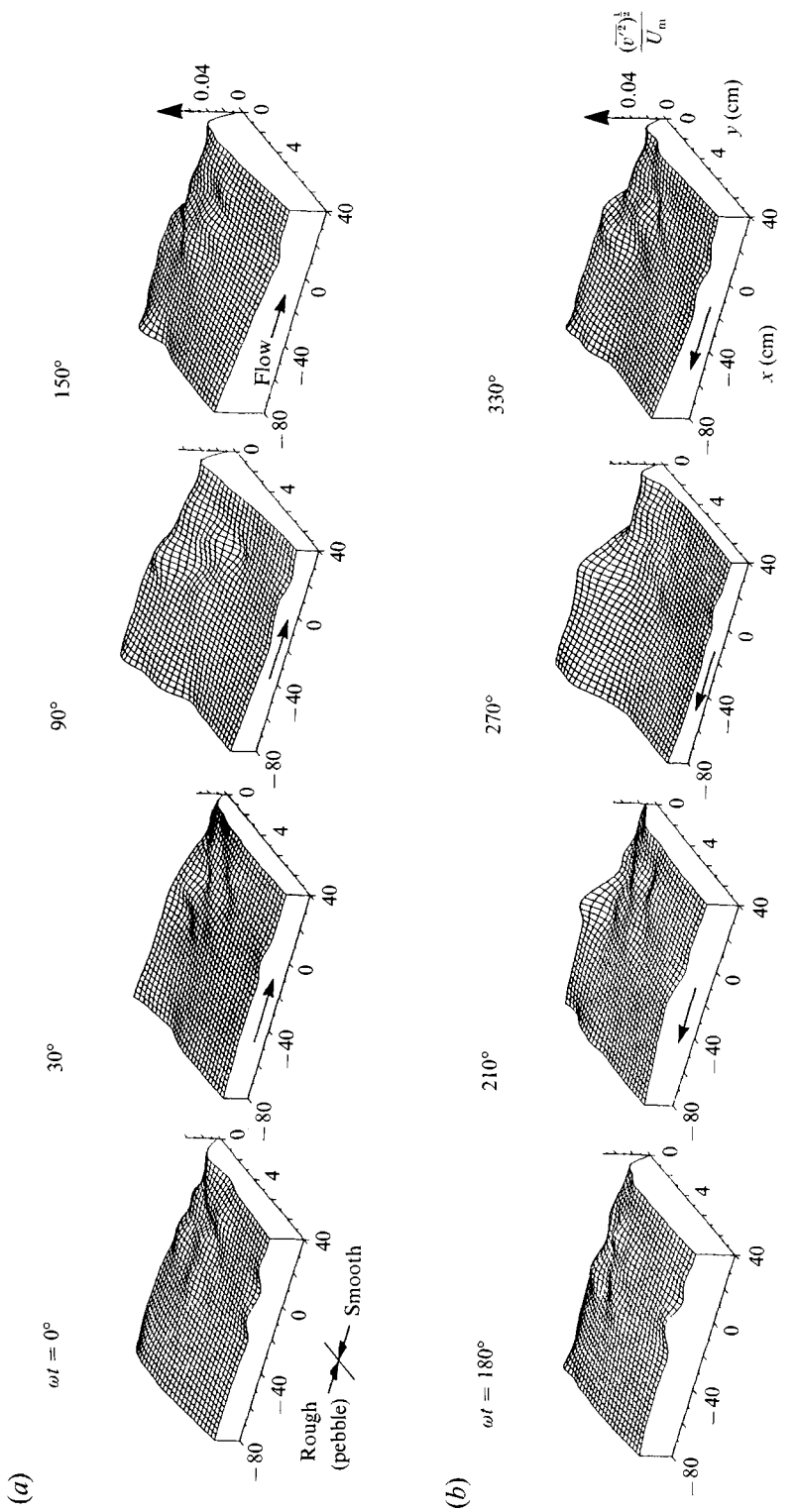

FIGURE 19. Root mean square value of v'. As figure 18.

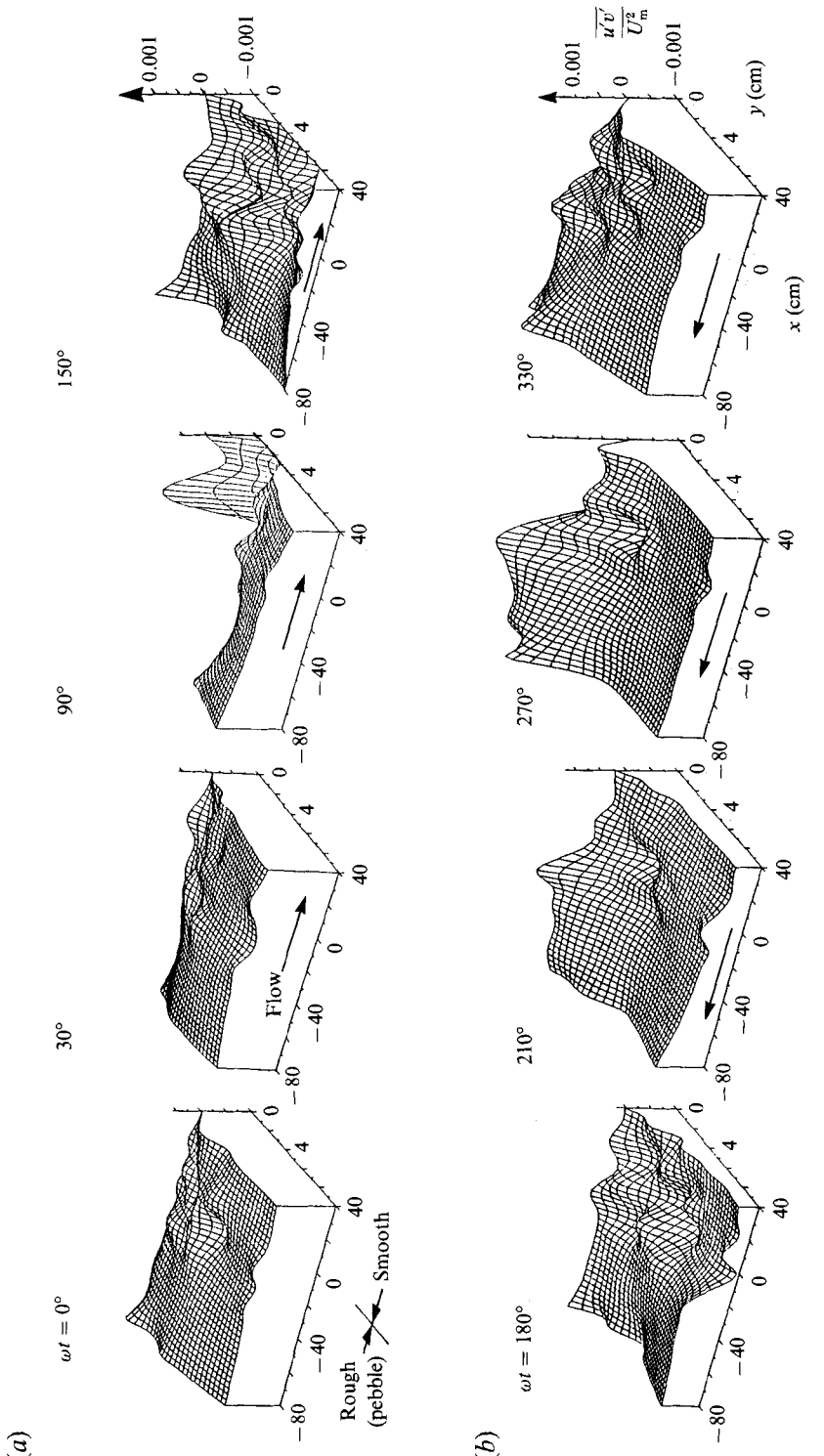

FIGURE 20. Reynolds stress $\overline{u'v'}$. As figure 18.

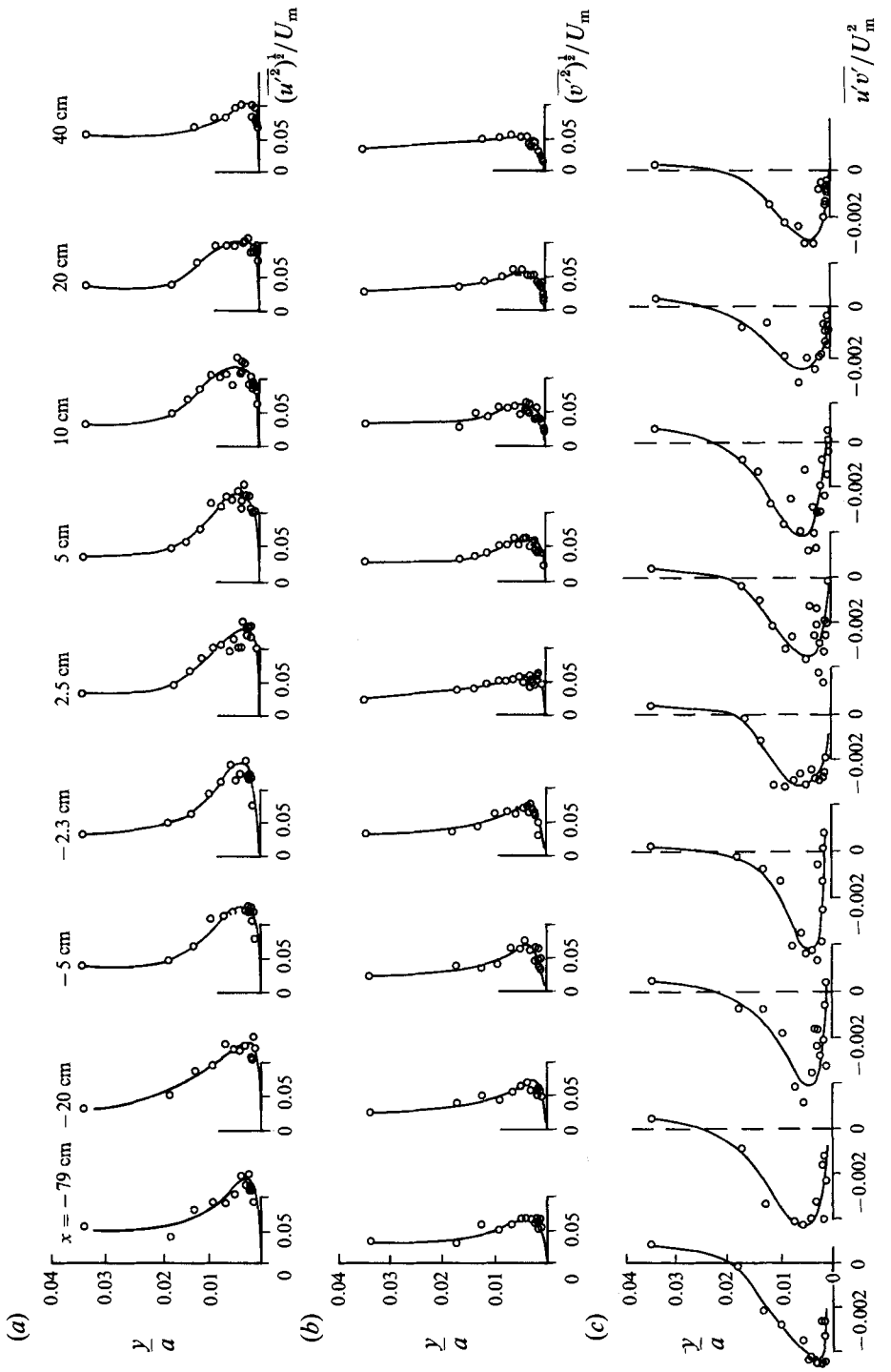

FIGURE 21. Turbulence quantities. $\omega t = 90°$. Flow from rough section (negative values of x locations) to smooth section (positive values of x locations). Test series 1.

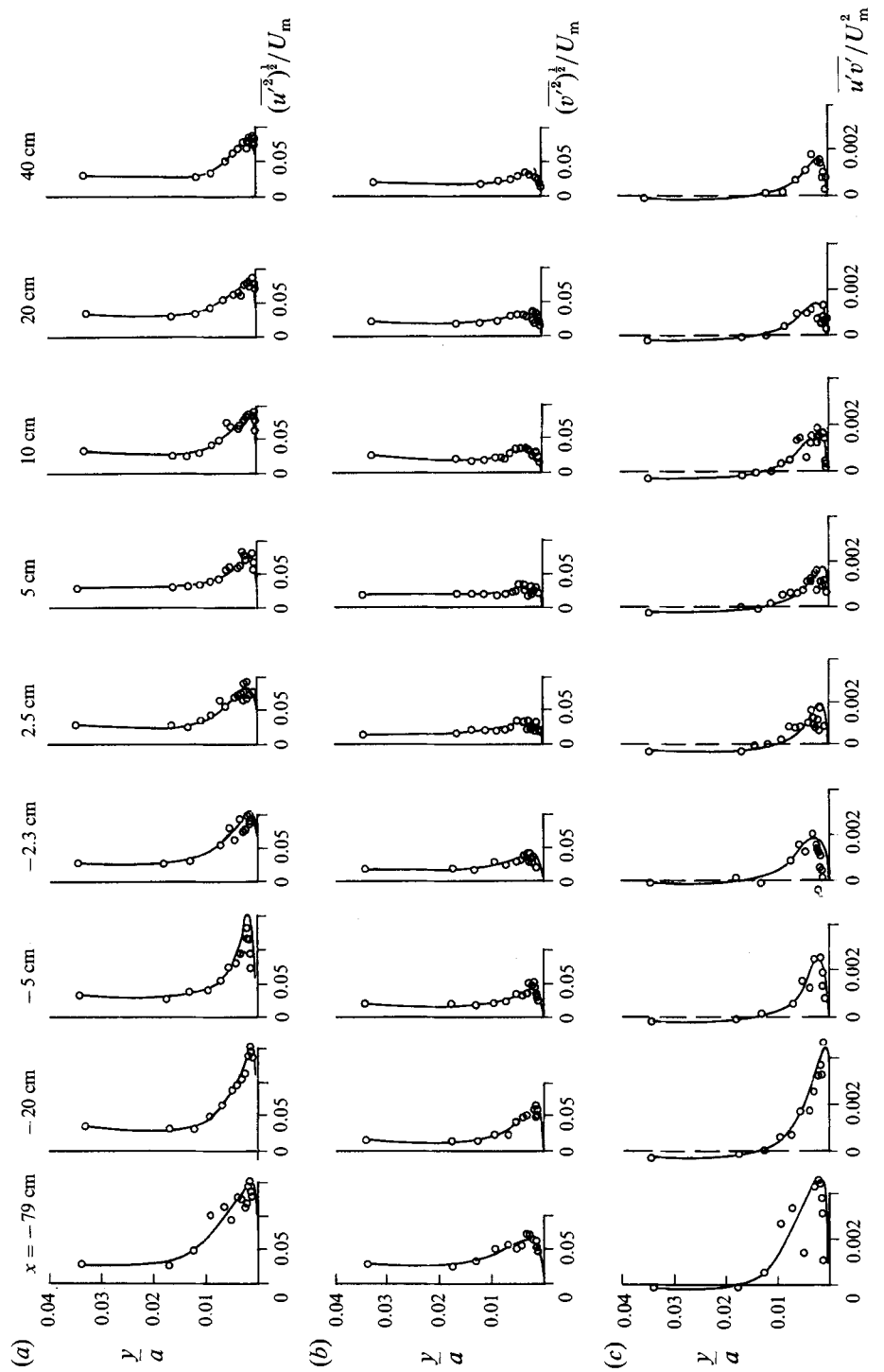

FIGURE 22. Turbulence quantities. $\omega t = 270°$. Flow from smooth section (positive values of x locations) to rough section (negative values of x locations). Test series 1.

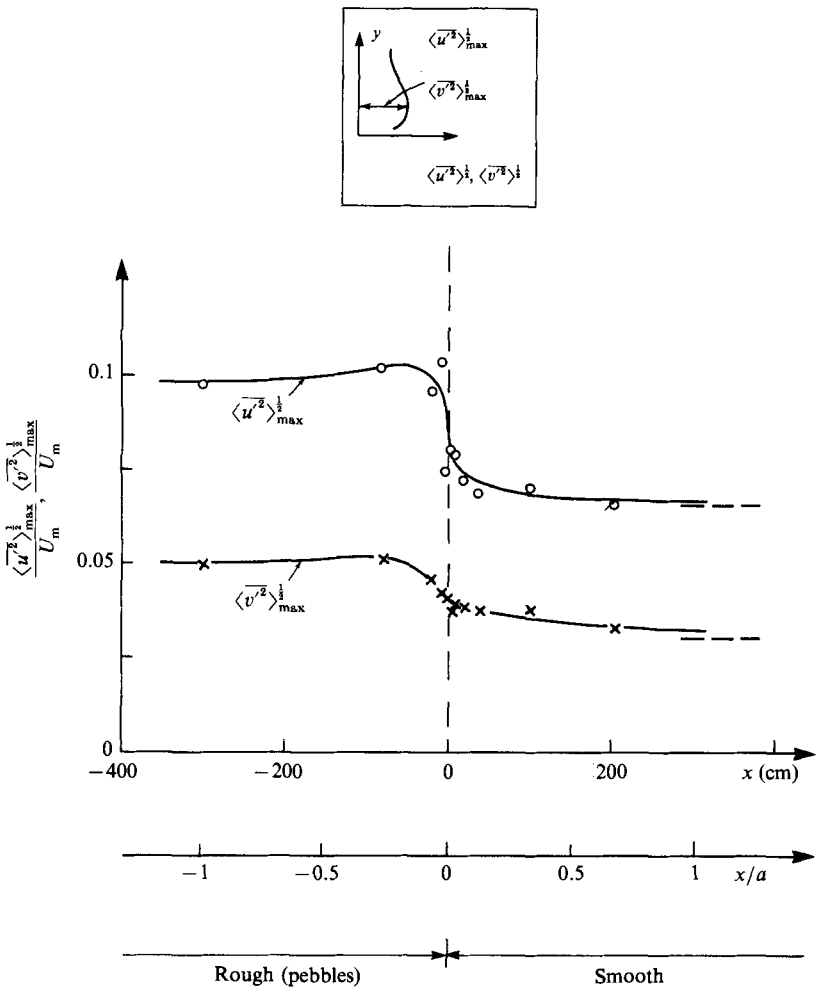

FIGURE 23. Peak values of period-averaged turbulence intensities. Test series 1 (rough (pebbles)/smooth). Asymptotic values: from Jensen *et al.* (1989).

of the large roughness section. Figure 14 further indicates that the streaming near the bed is balanced by a flow in the opposite direction at higher elevations from the bed.

The streaming can be explained as follows: consider the test series 1 situation, and consider an observer sitting at a point just above the bed at the rough-bed section in the neighbourhood of the junction between the two bed sections. This observer will experience velocities which are relatively higher in the smooth-to-rough half period than in the rough-to-smooth half period. This obviously will result in a non-zero period-averaged velocity which is directed towards the rough-bed section near the bed.

The effect which creates the streaming will apparently decrease with the distance from the junction between the two bed sections. This is in fact quite clear from figure 14. This implies that there should be a counter flow at higher elevations, directed towards the smooth-bed section, to satisfy the continuity. The latter means that a recirculating flow pattern should exist over the length of the bed where the streaming occurs. Figure 15, where the period-averaged resultant velocities are plotted in the form of a vector diagram for test series 3, clearly reveals this. Figure 14, on the other

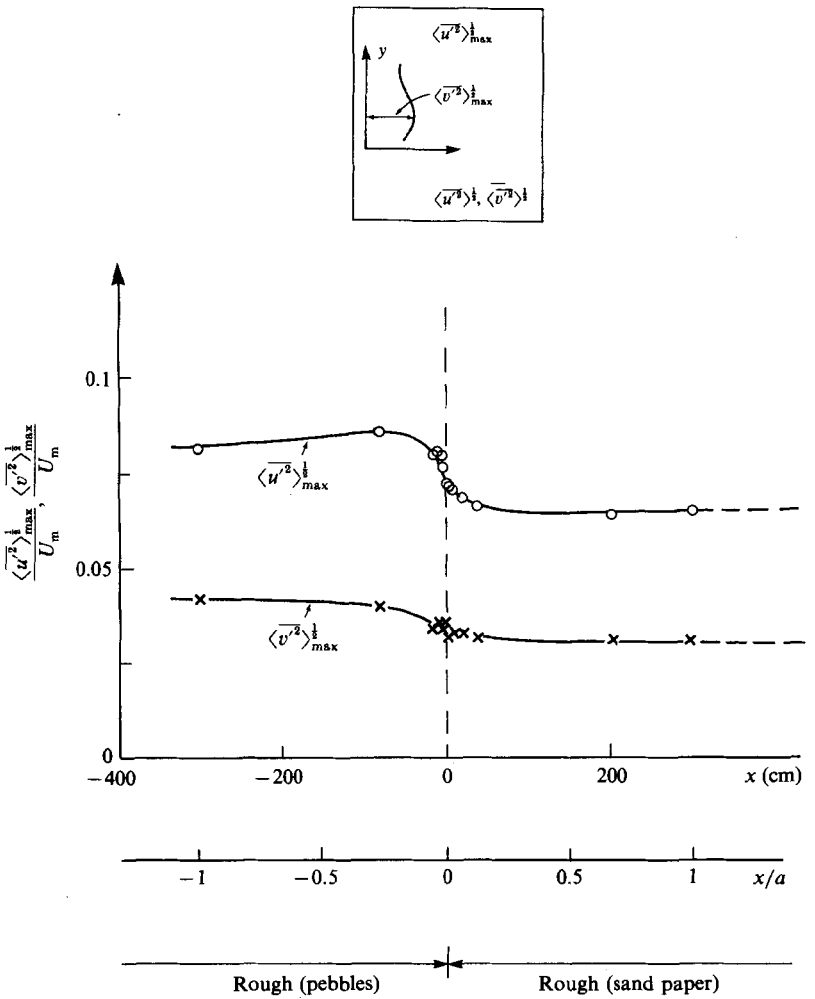

FIGURE 24. Peak values of period-averaged turbulence intensities. Test series 3 (rough (pebbles)/rough (sand-paper)). Asymptotic values: from Jensen *et al.* (1989).

hand, indicates that the streaming can be felt as far away from the junction between the two bed sections as $x = -80$ cm ($x/a = -0.25$).

Returning to figure 15, one interesting feature exhibited in this figure is that there is a constant ejection of fluid from the bottom into the main body of the flow over the band $-15\text{ cm} \leqslant x < 0$. Figure 16 presents the mean vertical velocity profiles for the same test series as in the previous figure. The figure indicates that the ejection of fluid takes place during the half period where the flow is from the sand-paper section to the pebble section, and it further indicates that this occurs at phase values $180° < \omega t < 315°$ (indicated by arrows in the figure). Indeed, it is seen that at these phase values the vertical velocity near the bed has a very pronounced, positive, non-zero mean value over the band $-15\text{ cm} \leqslant x < 0$. The figure further shows that this non-zero mean value could be as large as 10% of U_m, i.e. as large as approximately 20 cm/s, taking $U_m \approx 2$ m/s (see table 1, test series 3). It should be noted that the entrainment of the bottom fluid into the main body of the flow at the location where the roughness

changes can be seen very clearly from the flow visualization photograph presented in LHermitte (1958).

An obvious consequence of this phenomenon, namely the constant ejection of bottom fluid into the flow, is the generation of additional bed friction owing to the retarding effect of the ejected bottom fluid on the stream. This explains why the bed shear stress increases and attains a peak value near $x = 0$ over the pebble bed section before it relaxes to its asymptotic value as $x \to -\infty$ (figures 7*b* and 8*b*). The relatively weak peaks observed in figures 7(*a*) and 8(*a*) can be explained in the same way as in the preceding, where the occurrence of the peak can be linked to the positive non-zero vertical mean velocities experienced at $\omega t = 45°$, 90° and 135° at $x = 5$ cm in figure 16(*a*) (indicated by arrows in the figure).

The occurrence of the non-zero mean vertical velocities itself, on the other hand, may be attributed to the local adverse pressure gradient created in the neighbourhood of the junction between the two bed sections owing to the abrupt change in the roughness.

Finally, figure 17 shows the variation of the maximum value of the streaming velocity. The latter, when normalized by the velocity amplitude U_m, is expected to be a function of k_s/k_s' and a/k_s. The figure exhibits this variation as a function of the roughness ratio k_s/k_s' for $a/k_s = 60$ and 200. The streaming velocities plotted in the figure were corrected for the existing streaming in the tunnel indicated in figure 13, by simply subtracting the latter from the measured streaming.

6. Turbulence quantities

Figures 18–20 present the turbulence data at different phases for test series 1. At $\omega t = 0°$ it is seen that turbulence is more or less evenly distributed in the tunnel. This turbulence is the reminiscence of the turbulence from the previous half period. As the flow progresses during the half period from $\omega t = 0°$ to 180°, more and more turbulence is generated near the bed and brought into the free-stream region. As the half period comes to an end ($\omega t = 180°$), again the turbulence becomes more or less evenly distributed over the (x, y)-plane. Things develop in a similar way in the next half period.

From Figures 18–20 three points can be noted: (i) the turbulence left in the tunnel at the end of the rough-to-smooth half period (i.e. at $\omega = 180°$) is distinctly larger than that at the end of the smooth-to-rough half period (i.e. at $\omega t = 0°$); (ii) the turbulence over the rough-bed section is always larger than that over the smooth-bed section; (iii) the turbulence experienced through the two half periods is not necessarily the same.

Figure 21 gives a detailed illustration of the streamwise variation of turbulence at $\omega t = 90°$, while figure 22 gives that for $\omega t = 270°$, both for test series 1. At $\omega t = 90°$, the flow is from the pebble-bed section to the smooth-bed section, while at $\omega t = 270°$ it is in the opposite direction. The figures indicate that the turbulence distributions relax to their asymptotic distributions over a transition length, which extends from the junction between the two bed sections ($x = 0$) to approximately $x = +20$ cm ($x/a = +0.07$) for the flow at $\omega t = 90°$ (figure 21) and from $x = 0$ to approximately $x = -20$ cm ($x/a = -0.07$) for the flow at $\omega t = 270°$ (figure 22).

Finally, figures 23 and 24 present the period-averaged turbulence data, namely $\langle \overline{u'^2} \rangle^{\frac{1}{2}}_{max}$ and $\langle \overline{v'^2} \rangle^{\frac{1}{2}}_{max}$, for the rough (pebbles)/smooth transition and the rough (pebbles)/rough (sand paper) transition, respectively. The present results agree with the results obtained by Jensen *et al.* (1989) for large values of $+x$, as seen from the figures.

One interesting feature from these figures is that the turbulence over the pebble bed

section appears to be larger in the rough (pebbles)/smooth bed experiments than in the rough (pebbles)/rough (sand paper) ones. This may be attributed to the fact that the dispersion of turbulence across the depth would be larger in the case of rough (pebbles)/rough (sand paper) bed experiments, thus the peaks in the variation of $\langle\overline{u'^2}\rangle^{\frac{1}{2}}$ and $\langle\overline{v'^2}\rangle^{\frac{1}{2}}$ over the depth are smoothed out, therefore smaller values are measured for $\langle\overline{u'^2}\rangle^{\frac{1}{2}}_{\max}$ and $\langle\overline{v'^2}\rangle^{\frac{1}{2}}_{\max}$.

7. Summary and conclusions

(i) The response of the bed shear stress to a sudden change in the bed roughness occurs over a transitional length along the bed.

(ii) The bed shear stress over this transitional length attains a peak over the bed section with larger roughness. This peak occurs rather close to the junction where the roughness change takes place.

The magnitude of the peak is different in the two half periods; it is larger in the half period where the flow is towards the bed section with the larger roughness.

The peak bed shear stress ranges from 1 (the homogeneous bottom roughness) to 2.5 times the undisturbed value. It was found that this peak value of the bed shear stress is about 2.5 times the undisturbed value over the pebble bed section in the case of the pebble-bed/smooth-bed experiment, while this figure is 1.8 in the case of the pebble-bed/sand-paper-bed experiment of the present study.

It may be mentioned that the steady theory predicts the peak shear stress rather well.

(iii) There exists a streaming near the bed in the direction towards the bed section with the larger roughness. The most intensive streaming occurs in the neighbourhood of the junction where the roughness change takes place.

It was found that the streaming is felt as far away from the junction between the two bed sections as $x = -80$ cm ($x/a = -0.25$) for the tests conducted in the present study, x being the distance from the section where the roughness changes.

(iv) Regarding the turbulence quantities, the response of the turbulence quantities to the sudden change in roughness occurs again over an area. It was found that this transitional area extends from $x/a \approx -0.07$ to $x/a \approx +0.07$ at the phase values $\omega t = 90°$ and $270°$ for the pebble-bed/smooth-bed experiment of the present study.

(v) The turbulence is quantitatively different in the two half periods; it is stronger in the half period where the flow is towards the less-rough section.

The study is partially supported by the research programme 'Marine Technique' of the Danish Scientific Council (STVF) and by the Commission of the European Communities, Directorate General for Science, Research and Development, under MAST contracts no. 0035-6 and MAS 2 CT 92-0027.

REFERENCES

ANDREOPOULOS, J. & WOOD, D. H. 1982 The response of a turbulent boundary layer to a short length of surface roughness. *J. Fluid Mech.* **118**, 143–164.

ANTONIA, R. A. & LUXTON, R. E. 1971 The response of a turbulent boundary layer to a step change in surface roughness. Part 1. Smooth to rough. *J. Fluid Mech.* **48**, 721–761.

ANTONIA, R. A. & LUXTON, R. E. 1972 The response of a turbulent boundary layer to a step change in surface roughness. Part 2. Rough to smooth. *J. Fluid Mech.* **53**, 737–757.

BAKKER, W. T. 1974 Sand concentration in an oscillatory flow. *Proc. 14th Conf. Coastal Engng Copenhagen*, pp. 1129–1148.

BAYAZIT, M. 1976 Free surface flow in a channel of large relative roughness *J. Hydraul. Res.* **14**(1), 115–126.

BELCHER, S. E., XU, D. P. & HUNT, J. C. R. 1990 The response of a turbulent boundary layer to arbitrarily distributed two-dimensional roughness changes. *Q. J. R. Met. Soc.* **116**, 611–635.

BRADLEY, W. F. 1968 A micrometeorological study of velocity profile and surface drag in the region modified by a change in surface roughness. *Q. J. R. Met. Soc.* **94**, 361–379.

FREDSØE, J. 1984 Turbulent boundary layer in wave-current motion. *J. Hydraul. Engng ASCE* **110**, 1103–1120.

GRANT, W. D. & MADSEN, O. S. 1979 Combined wave and current interaction with a rough bottom. *J. Geophys. Res.* **84**(C4), 1797–1808.

HAGATUN, K. & EIDSVIK, K. J. 1986 Oscillating turbulent boundary layers with suspended sediment. *J. Geophys. Res.* **91**(C11), 13045–13055.

HINO, M., KASHIWAYANAGI, M., NAKAYAMA, A. & HARA, T. 1983 Experiments on the turbulence statistics and the structure of a reciprocating oscillatory flow. *J. Fluid Mech.* **131**, 363–400.

JENSEN, B. L. 1989 Experimental investigation of turbulent oscillatory boundary layers. Thesis, Technical University of Denmark, Institute of Hydrodynamics and Hydraulic Engineering, Lyngby, Denmark.

JENSEN, B. L., SUMER, B. M. & FREDSØE, J. 1989 Turbulent oscillatory boundary layers at high Reynolds numbers. *J. Fluid Mech.* **206**, 265–297.

JUSTESEN, P. 1988 Prediction of turbulent oscillatory flow over rough beds. *Coastal Engng* **12**, 257–284.

JUSTESEN, P. & FREDSØE, J. 1985 Distribution of turbulence and suspended sediment in the wave boundary layer. *Prog. Rep.* **62**, 61–67. Inst. of Hydrodyn. & Hydraul. Engng, Technical University, Denmark.

KAJIURA, K. 1968 A model for the bottom boundary layer in water waves. *Bull. Earthquake Res. Inst.* **45**, 75–123.

LHERMITTE, M. P. 1958 Contribution à l'étude de la couche limite des houles progressives. Ministère de la Défense Nationale Secrétariat d'État à la Marine. Comité Central D'Océanographie et D'Étude de Côtes. No. 136.

LONGUET-HIGGINS, M. S. 1957 The mechanics of the boundary-layer near the bottom in a progressive wave. Appendix to R. C. H. Russell & J. C. C. Osorio, An experimental investigation of drift profiles in a closed channel. *Proc. 6th Intl Conf. Coastal Engng Miami, Florida*, pp. 184–193.

SLEATH, J. F. A. 1987 Turbulent oscillatory flow over rough beds. *J. Fluid Mech.* **182**, 369–409.

SPALART, P. R. & BALDWIN, B. S. 1987 Direct simulation of a turbulent oscillating boundary layer. *NASA Tech. Mem.* 89460, Ames Research Center, Moffett Field, CA. (Also in *Turbulent Shear Flows 6*, Springer.)

SPALART, P. R. & LEONARD, A. 1987 Direct numerical simulation of equilibrium turbulent boundary layers. In *Turbulent Shear Flows 5* (ed. F. Durst, B. E. Launder, J. L. Lumley, F. W. Schmidt & J. H. Whitelaw), pp. 234–252. Springer.

SUMER, B. M., LAURSEN, T. S. & FREDSØE, J. 1993 Wave boundary layers over a sloping bed. *Coastal Engng* (submitted).

TOWNSEND, A. A. 1966 The flow in a turbulent boundary layer after a change in surface roughness. *J. Fluid Mech.* **26**, 255–266.

TSUJIMOTO, T., URUSHIZAKI, M. & MIYAGAKI, K. 1991 Turbulent flow with abrupt changes of roughness in open channels. KHL Communication, Hydraulics Lab. Dept. Civil Engineering, Kanazawa University, Japan, *Progressive Res. Rep.*/June 1991, pp. 59–78.